Dioscin-mediated autophagy alleviates neuronal degeneration in MPP+-treated SH-SY5Y of Parkinson's disease model

Shofiul Azam [1], Md. Ezazul Haque [1], Duk-Yeon Cho [1], JoonSoo Kim [1], Md. Jakaria [3], In-Su Kim [2], Dong-Kug Choi [1, 2*]

[1] Department of Applied Life Science & Integrated Bioscience, Graduate School, BK21 Program, Konkuk University, Chungju 27478, Korea; shofiul_azam@hotmail.com (SA); mdezazulhaque@yahoo.com (MEH); whejrdus10@kku.ac.kr (DYC); kgfdkr@gmail.com (JSK)

[2] Department of Integrated Bioscience & Biotechnology, College of Biomedical and Health Science, Research Institute of Inflammatory Disease (RID), Konkuk University, Chungju 27478, Korea; kis5497@hanmail.net (ISK)

[3] Melbourne Dementia Research Centre, The Florey Institute of Neuroscience and Mental Health, The University of Melbourne, Parkville, VIC, 3052, Australia; md.jakaria@florey.edu.au (MJ)

*Correspondence: choidk@kku.ac.kr; Tel.: +82-43-840-3610; Fax: +82-43-840-3872

Abstract

Autophagy is a cellular homeostatic process by which cells degrade and recycle their malfunctioned contents, and impairment in this process leads to Parkinson's disease (PD) pathogenesis. Dioscin, a steroidal saponin, has induced autophagy in several cell lines and animal models. The role of dioscin-mediated autophagy in PD remains to be investigated. Therefore, this study aims to investigate the hypothesis that dioscin-regulated autophagy and autophagy-related genes (ATG) could protect neuronal cells in PD via reducing apoptosis and enhancing neurogenesis. In this study, the 1-methyl-4-phenylpyridinium ion (MPP^+) were used to induce neurotoxicity and impair autophagic flux in a human neuroblastoma cell line (SH-SY5Y). The result showed that dioscin pre-treatment counters MPP^+-mediated autophagic flux impairment and alleviates MPP^+-induced apoptosis by downregulating activated caspase-3 and Bax expression while increasing Bcl-2 expression. In addition, dioscin pre-treatment was found to increase neurotrophic factors and tyrosine hydroxylase expression, suggesting that dioscin could ameliorate MPP^+-induced degeneration in dopaminergic neurons and benefit the PD model. Interestingly, the neuroprotective activities of dioscin were suppressed when co-treated with chloroquine (CQ), an autophagosome-lysosome inhibitor. In summary, we showed dioscin's neuroprotective activity in neuronal SH-SY5Y cells might be partly related to its autophagy induction and suppression of the mitochondrial apoptosis pathway.

Keywords: *MPP^+; neurotoxicity; autophagy; apoptosis; neuroprotection; Parkinson's disease*
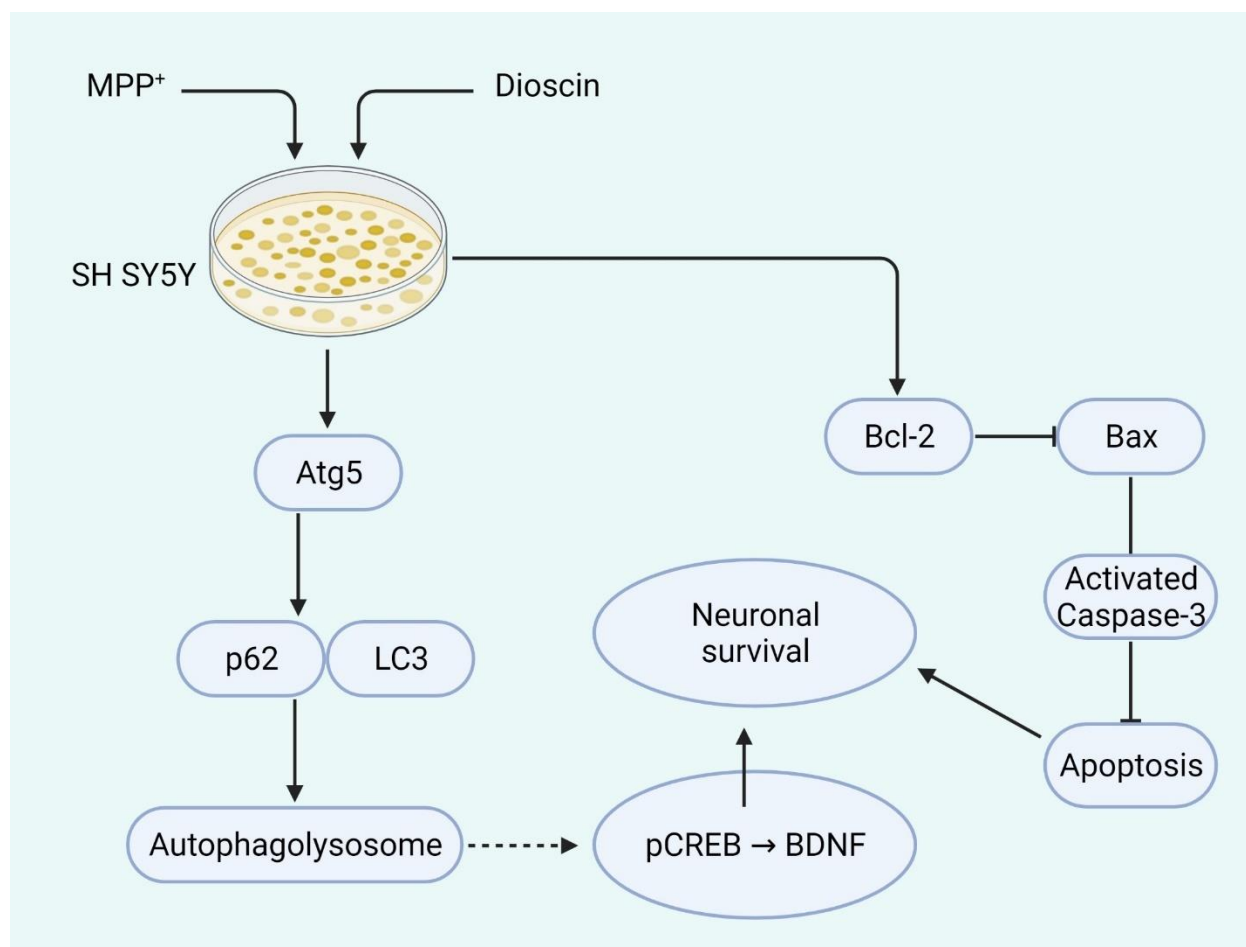
Fig: Graphical abstract

Introduction

Parkinson's disease (PD) is one of the most prevalent age-related neurodegenerative diseases that is characterised by the loss of dopaminergic neurons in the substantia nigra pars compacta (SNpc), the formation of intraneuronal proteinaceous inclusion and Lewy bodies [1,2]. Although the exact etiology of PD is still not clear, evidence suggests that mitochondrial dysfunction and oxidative stress plays a major role in PD pathogenesis [3].

1-methyl-4-phenylpyridinium ion (MPP$^+$) is an active metabolite form of 1-methyl-4-phenyl-1,2,3,6-tetrahydropyridine (MPTP) [4,5], which is a common neurotoxin used to establish *in vitro*

PD model in human dopaminergic cell lines such as SH-SY5Y neuroblastoma cells. MPP$^+$ translocates through the dopaminergic neurons by the dopamine transporter (DAT), leading to the inhibition of mitochondrial complex I and ATP synthesis and increases in reactive oxygen species (ROS), ultimately, causes neuronal degeneration [6].

Autophagy is a cellular homeostatic process by which intracellular components, including damaged organelles, misfolded or aggregated proteins, and intracellular pathogens, degrade into the cytoplasm of the cell [7,8]. In the autophagic process, a double-membrane vesicle, the autophagosome, forms that deliver targeted cellular components to lysosome and fuse within to form autolysosome, which can degrade and recycle malfunctioned contents of cells. Autophagy is a homeostatic process of the cell, while its impairment contributes to various disease pathology. This process can be considered a stress response of cells that promotes cell survival; contrarily, autophagy dysfunction could promote cell death [9], leading to neurodegenerative diseases, cancer and ageing-related diseases [10]. Several studies showed that autophagic dysfunction, such as clearance of mutant α-synuclein, is involved in the pathogenesis of PD [2,11,12]. MPP$^+$ can increase the microtubule-associated protein light-chain 3 (LC3)-II/LC3-I expressions, a major marker of autophagy, in SH-SY5Y cells [13], but prolonged exposure to MPP$^+$ reduces the LC3 expression, as chronic exposure to MPP$^+$ impairs autophagosome [14] by lowering phagophore [15].

Dioscin is a steroidal saponin (**Fig. 1**), abundant in several medicinal plants, including *Diosocorea nipponica* Makino and *Diosocorea rizhoma*, and it is widely used to synthesise hormonal drugs [16]. Dioscin is also an important raw material of Chinese traditional medicine and is famous for aging-related diseases such as AD [17,18] and activities such as anti-inflammation, anti-tumour and anti-allergy [17]. Previous reports showed dioscin-induced autophagy mitigates cell apoptosis

via phosphatidylinositol 3-kinase (PI3K)/protein kinase B (Akt) pathway [16], alleviates pulmonary inflammation and fibrosis [19]. This steroidal saponin also showed neuroprotective effects in a rat model of cerebral ischemia/reperfusion [20], improved neurogenesis by promoting 5-HT metabolism [21] and can improve spatial learning memory in ischemic mice [22]. In recent studies, dioscin was found to be ameliorated brain aging by reducing oxidative stress and inflammation [18] and induced autophagy to protect against $A\beta_{1-42}$-induced neurotoxicity in HT22 cells [17].

Although the molecular mechanism of autophagic involvement in neurogenesis via regulating neurotrophic factors is fully not revealed, recent studies suggest that MPP^+ precursor MPTP treatment causes partial deficiency of autophagy-related gene 5 (ATG5) [23] in PD that causes accumulation of PD proteins in dopaminergic neurons, leading to apoptosis and downregulation of neurogenesis factors [23]. Mitochondrial dysfunction also impairs ATG5-dependent autophagy and causes dopaminergic cell death via caspase-3 activation [15]. ATG5 is considered a key regulator of autophagic vacuoles and autophagy level [24]; ATG5 upregulation increases LC3I/II conversion by reducing p62/sequesterosome-1 [23]. We, therefore, speculate that dioscin could prevent ATG5 deficiency, resulting in dopaminergic neuron transcription factors enhancement and dopaminergic neurogenesis via increased expression of neurotrophic factors. We also hypothesise that dioscin-mediated autophagosome restoration would reduce apoptosis, alleviate neuronal survival and protect damage in a dopaminergic cell line.
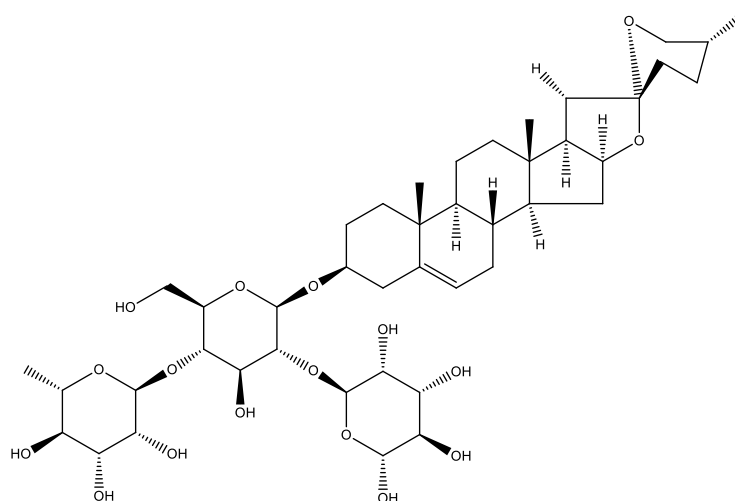
Figure 1: Chemical structure of dioscin

Results

Dioscin protects against neurotoxicity

Different concentrations of MPP$^+$ (250–2000 μM) was induced to SH-SY5Y cells and incubated

for 24 h to select the optimal dose of MPP$^+$. The cell survivability was dose-dependently reduced

by MPP$^+$ treatment (Fig. 2A). Our results relate to previous findings [25,26] and clearly showed

that the optimal concentration of MPP$^+$ is 1 mM. The 1 mM dose was selected to establish an *in*

vitro PD model [26] and further experiment. Similarly, the optimal concentration of CQ to be used

for this study was screened by MTT assay (Fig. 2B). Although MTT assay showed CQ 40 μM is

quite toxic to cells [27,28], our dose-dependent (CQ) immunoblotting assay showed this dose is

better suited to inhibit autophagic flux (Suppl. 1). Hence, CQ 40 μM was selected for subsequent

study. Dioscin dose-dependently, except at the dose of 800 ng/mL [18], reduced MPP$^+$ activity

and increased cells viability; therefore, 100 – 400 ng/mL of dioscin dose was selected for

subsequent study (Fig. 2C). Dioscin at that prescribed doses also affected cell viability

substantially in LPS-induced BV2 cells and H$_2$O$_2$-treated PC12 cells (Suppl. 2A & B). Dioscin

6

also alleviated inflammatory cytokines released in response to LPS in microglial BV-2 cells (Suppl. 3). MPP^+-induced apoptosis on SH-SY5Y cells was also investigated by DAPI staining (Fig. 2E). MPP^+ treatment showed significant fragmentation of chromatin within the nucleus without changing nuclear phenotype. Pre-treatment of dioscin 200 and 400 ng/ml, but not 100 ng/ml, dose rescued neuronal cells from apoptotic death. Next, to evaluate the hypothesis of dioscin activity depending on autophagy, we co-treated CQ (40 μM) with dioscin (50 – 800 ng/ml) and MPP^+ (1 mM). Cell viability was significantly ([##]$p<0.001$) reduced after co-treatment of MPP^+ and CQ; inhibition of autophagy by CQ also reduced dioscin activity in SH-SY5Y cells and showed no significant protection (Fig. 2D). Dioscin's inability to protect neuronal cells in the presence of CQ (40 μM) was not because of CQ toxicity, to confirm that we assayed in the presence of 20 μM (Suppl. 4). Likewise, no protection was observed, which indicates that inhibition of the autophagic pathway restricts dioscin-mediated protection. This result indicates that dioscin might be depending on the autophagic pathway to improve neuronal cell survivability.
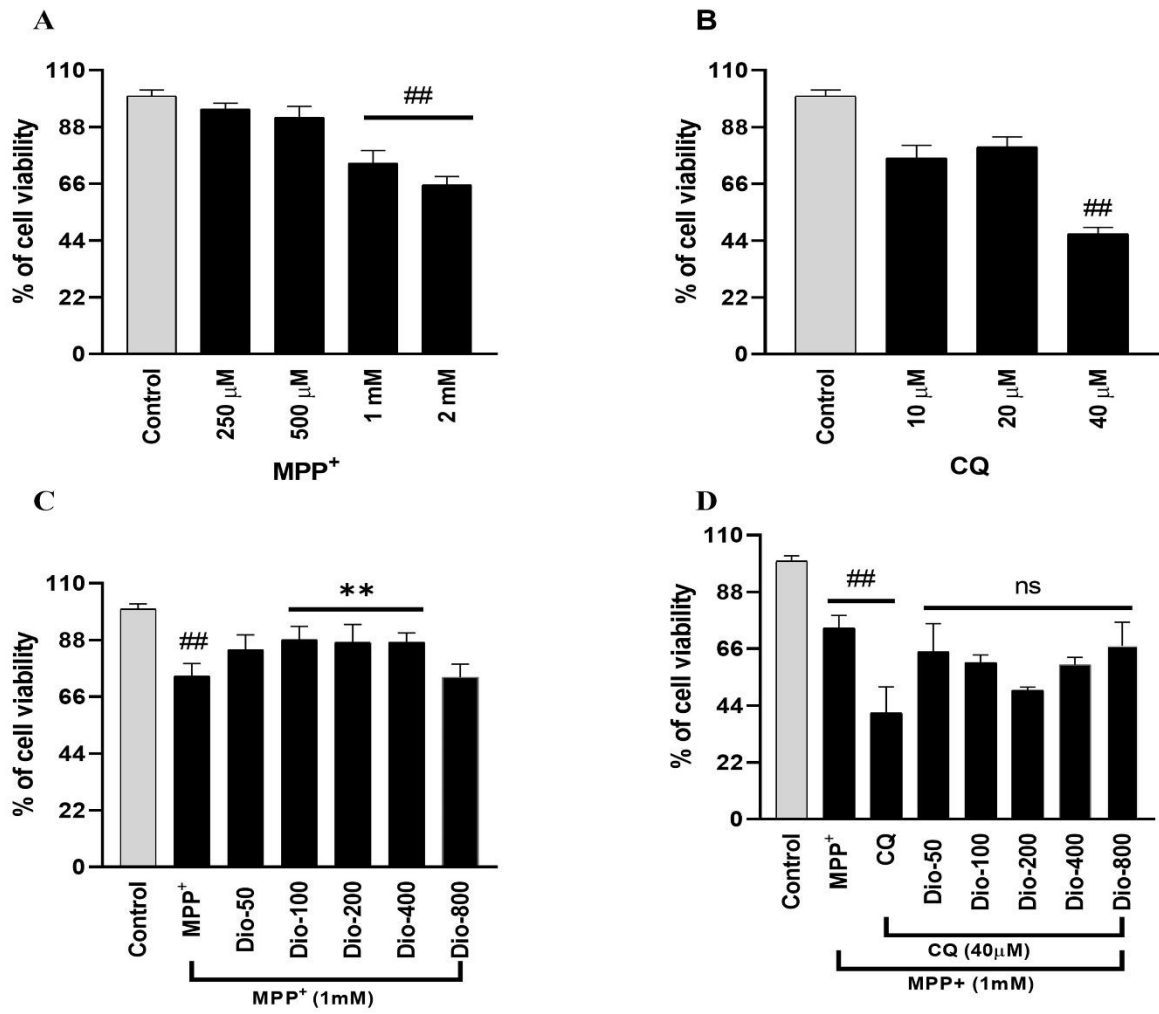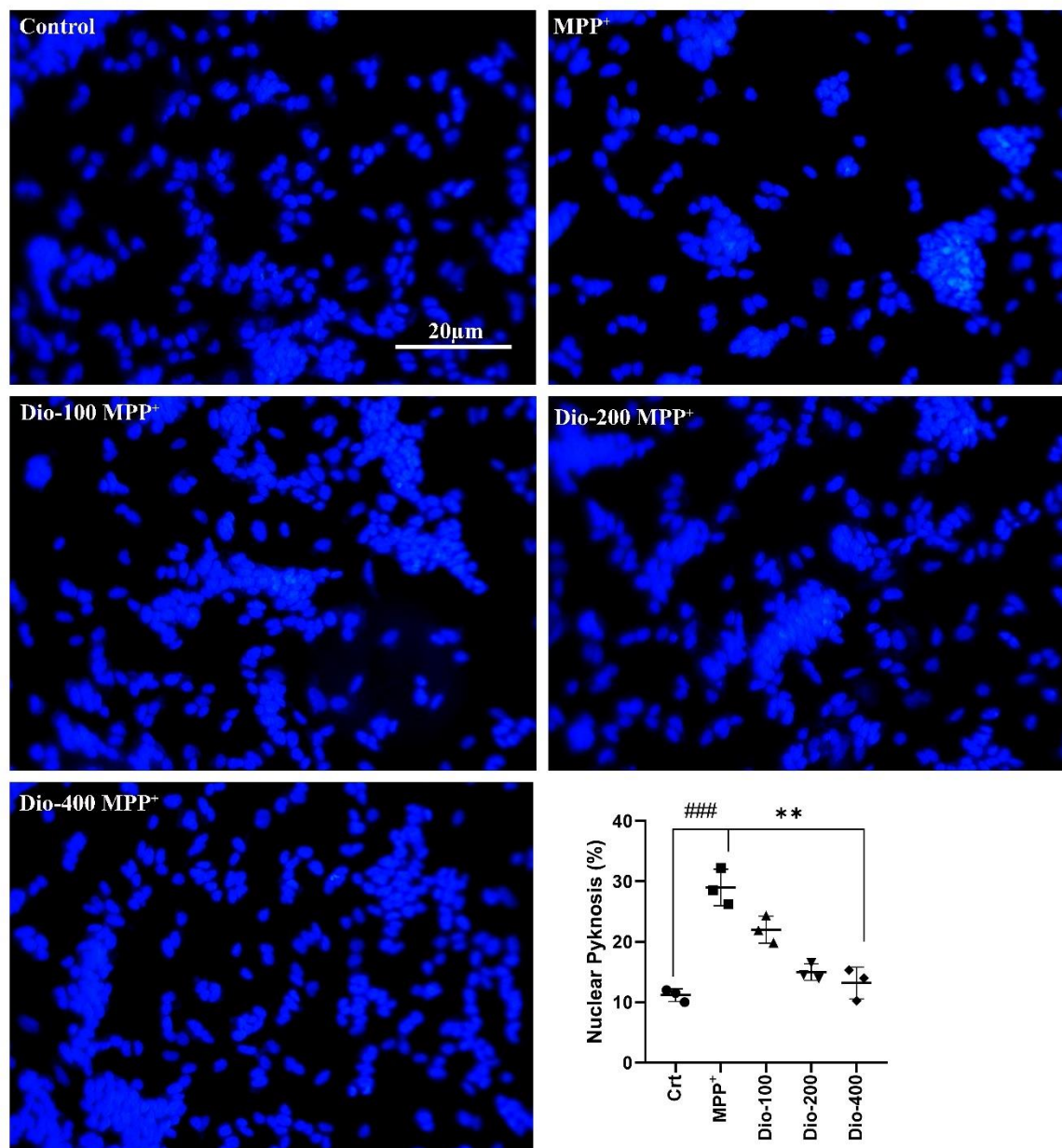
E

Figure 2: Evaluation of compounds on cell viability. (A) dose-dependent cell viability after MPP[+] treatment; (B) dose-dependent cell viability after chloroquine (CQ) treatment; (C) dose-dependent cell viability after co-treatment of dioscin and MPP[+] 1 mM; (D) dose-dependent cell viability of dioscin co-treated with MPP[+] (1 mM) and CQ (40 μM); (E) fluorescence microscopy

of SH-SY5Y cells stained with DAPI, white insides indicating chromatin aggregation; fluorescent images were taken with Nikon microscope (scale bar 20µm); calculations were done by scoring percent of cells with nuclear pyknosis in total stained ones using ImageJ software. Values are mean±SEM (n=3/group); ns= not significant; $^{\#}p<0.05$, $^{\#\#}p<0.01$ and $^{\#\#\#}p<0.001$, in comparison to non-treated group; $^{*}p<0.05$, $^{**}p<0.01$ and $^{***}p<0.001$, compared to toxin and treatment group.

Dioscin dose-dependently rescues autophagic function impaired by MPP$^+$

ATG5 is a crucial protein marker of autophagic vesicle formation. It has been reported that a decrease in ATG5 downregulates or inhibits autophagy, suggesting its central role in autophagy [29]. In agreement with a previous study [15], MPP$^+$ treatment substantially ($^{\#}p<0.05$) inhibited ATG5, indicating downregulation of autophagic flux formation, which was well supported by the up-regulation of LC3-adaptor protein SQSTM1/p62 (p62) (Fig. 3A). p62 is degraded by autophagy, and autophagic impairment results in the aggregation and up-regulation of this protein. Treatment with dioscin dose-dependently increased ATG5 in MPP$^+$-induced SH-SY5Y cells, while only 400 ng/mL dose substantially degraded p62 (Fig. 3A). To prove the hypothesis that dioscin affects autophagic flux formation, CQ, an autophagy inhibitor, was pre-treated 1 h before treating MPP$^+$ or MPP$^+$ and dioscin (100 – 400 ng/mL) in SH-SY5Y. The result showed significant ($^{\#}p<0.05$) impairment in MPP$^+$ and CQ treated group, and dioscin at high dose alone increased p62 degradation but no significant change observed in other two-dose (Fig. 3B). A similar potential effect of dioscin treatment was also evident in ATG5 expression (Fig. 3B).
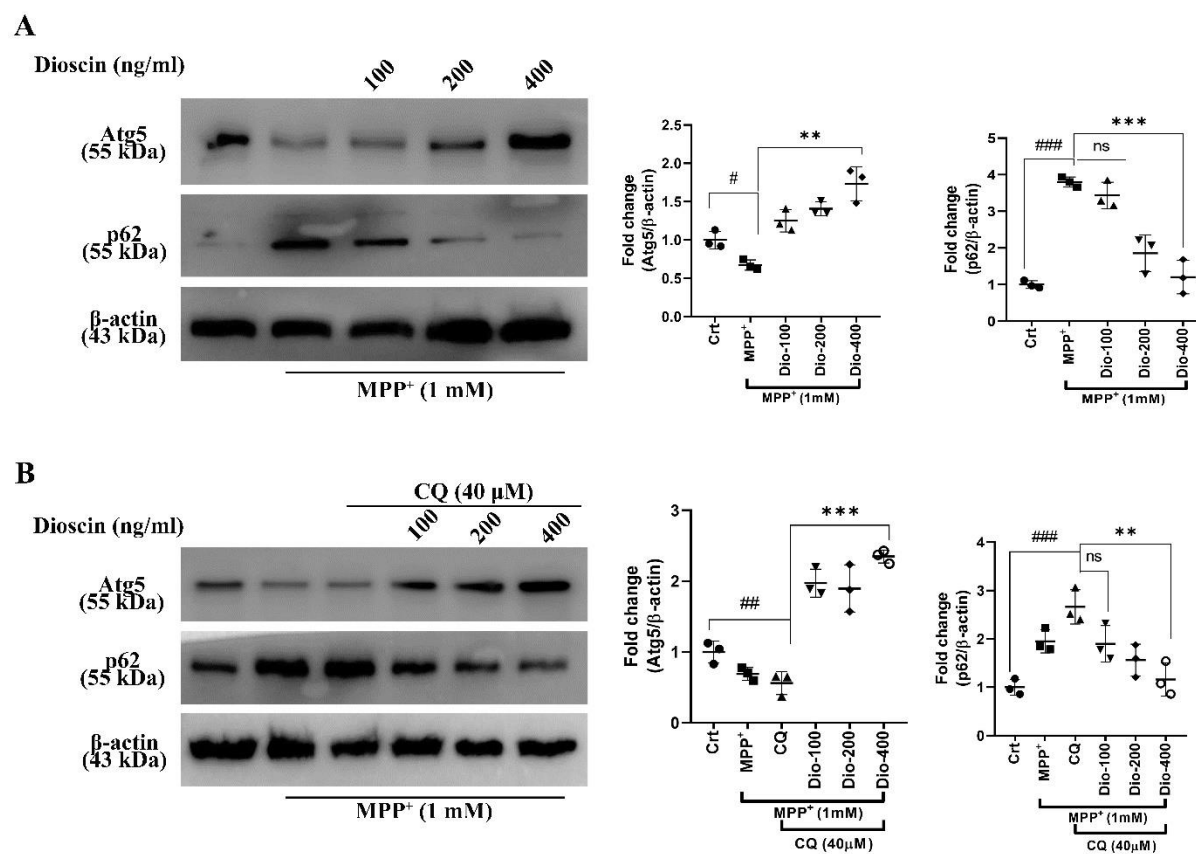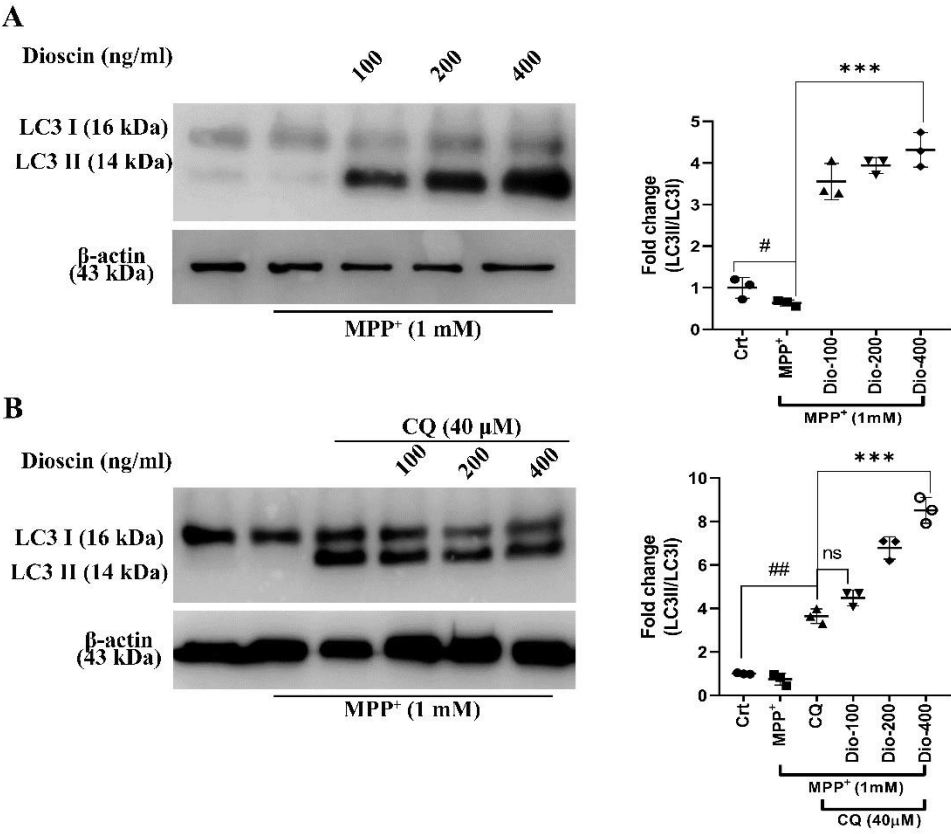
Figure 3: Dioscin dose-dependently activates autophagy. Representative data of ATG5 and p62 immunoblots of whole-cell (SH-SY5Y) lysates. ATG5 and p62 were used as an indicator of sequestosome formation. Cells were pre-treated with different doses of dioscin (**A**) and autophagy inhibitor CQ (40 μM) (**B**) followed by induction of MPP$^+$ (1mM). The optical density was measured using Image J software and presented as fold changes. Each WB is representative of 3 independent experiments. The bar graphs represent the ratio of respective protein/β-actin normalised against control (non-treated) samples or MPP$^+$ or MPP$^+$ +CQ-treated cells and are means ± SEM of 3 independent experiments. ns= not significant; $^{\#}$p<0.05, $^{\#\#}$p<0.01 and $^{\#\#\#}$p<0.001, in comparison to non-treated group; *p<0.05, **p<0.01 and ***p<0.001, compared to toxin and treatment group.

Dioscin dose-dependently upregulates autophagosome formation

Post-treated SH-SY5Y cell lysates were subjected to blot LC3, an autophagosome marker, to investigate the influence of dioscin pre-treatment on the autophagic response. On the activation of autophagy, LC3 is cleaved to form cytosolic LC3I, later converted into LC3II when conjugated to phosphatidylethanolamine [30]. Cells exposed to MPP$^+$ for 24 h showed impaired conversion into LC3II, indicating impaired autophagosome formation (Fig. 4A). Contrarily, the dioscin treatment group reversed that condition and significantly improved autophagosome formation supported by previous studies [16,19]. Cells were pre-treated with CQ (40μM) to justify the effect of dioscin on autophagic flux formation. Results showed CQ increased LC3 level, which is due to CQ capacity of impairing autolysosome degradation; treatment group at high dose have increased LC3 expression at least 3-fold than MPP$^+$ (Fig. 4B).

The dioscin-mediated autophagosome-lysosome fusion was further confirmed by fluorescence microscopy (Fig. 4C). Both treated and untreated SH-SY5Y cells were stained with an anti-LC3 antibody. Although it is not confirmed what phase of autophagy is blocked by MPP$^+$ chronic exposure, we speculated in agreement with previous findings [15] that MPP$^+$ might inhibit ATG5-dependent phagophore. So, MPP$^+$ treatment showed less fluorescence intensity after anti-LC3 exposure, indicating impairment of autophagosome. As an inhibitor of autophagosome-lysosome, CQ treatment increased LC3 puncta, which indicates inhibition of autophagic fusion. On the other hand, dioscin (400 ng/ml) treatment enhanced autophagic fusion (as seen in Fig. 4C) in MPP$^+$-treated SH-SY5Y, also reduced LC3 aggregation in CQ-cotreated cells.
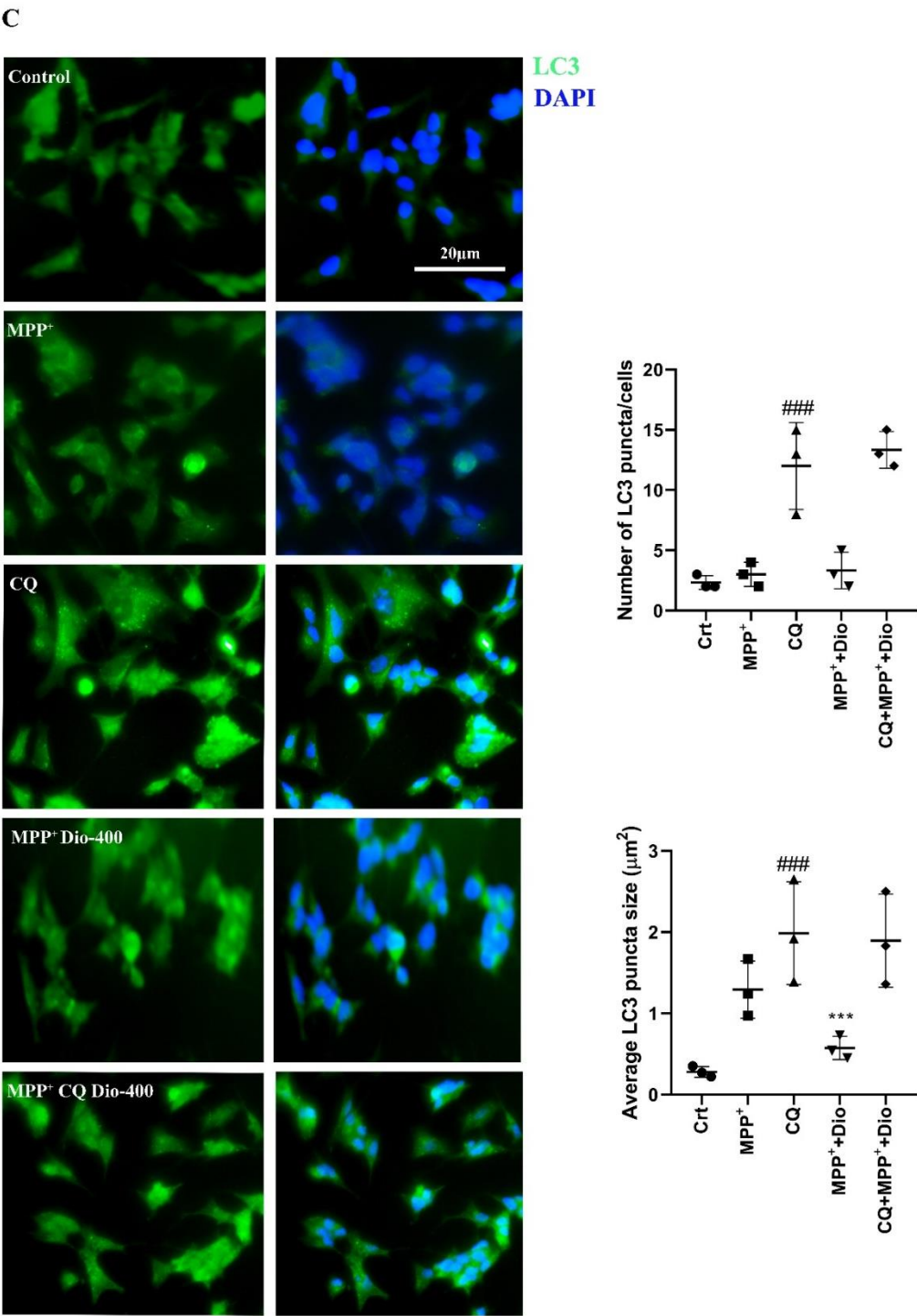
A

B

Figure 4: Dioscin dose-dependently activates autophagosome. Representative data of LC3 immunoblots of whole-cell (SH-SY5Y) lysates. Cells were pre-treated with different doses of Dioscin (**A**) and autophagy inhibitor CQ (40μM) (**B**) followed by induction of MPP$^+$ (1mM). The

conversion of LC3I into LC3II are presented as fold changes measured using Image J software. Each WB is representative of 3 independent experiments. Data in bar graphs represent the ratio of respective protein/β-actin or LC3I normalised against control (non-treated) samples or MPP$^+$ or MPP$^+$ +CQ-treated cells and are mean ± SEM of 3 independent experiments (**C**) Immunocytochemistry of autophagic marker LC3 in presence or absence of inhibitor CQ (40μM) on MPP$^+$-treated or untreated SH-SY5Y cells; red circles are indicating LC3 puncta; the images were taken by Nikon microscopy (20μm), and average size and number of LC3 puncta were done by ImageJ software; quantification performed from ≥25 cells. ns= not significant; [#]$p<0.05$, [##]$p<0.01$ and [###]$p<0.001$, in comparison to non-treated group; *$p<0.05$, **$p<0.01$ and ***$p<0.001$, compared to toxin and treatment group.

Dioscin dose-dependently downregulates apoptotic markers

In this part, we tested the effect of dioscin pre-treatment on apoptotic biomarkers, B-cell lymphoma 2 (Bcl-2), Bcl-2 associated X protein (Bax), caspase-3, and activated caspase-3 (cleaved caspase-3). Dioscin treatment dose-dependently reduced Bax expression (Fig. 5A), in contrast, increased Bcl-2 expression. Similarly, dioscin dose-dependently reduced caspase-3/ cleaved caspase-3 ratio (Fig. 5C). However, this protective activity was substantially affected by blocking the autophagic pathway. In the presence of CQ (40μM), dioscin did not reduce Bax and cleaved caspase-3 expression significantly (Fig. 4B & 5D), neither improve Bcl-2 expression (Fig. 5B). This modulation in activity shows that dioscin was shown to protect against MPP$^+$-induced toxicity by inducing mitochondrial autophagic clearance.
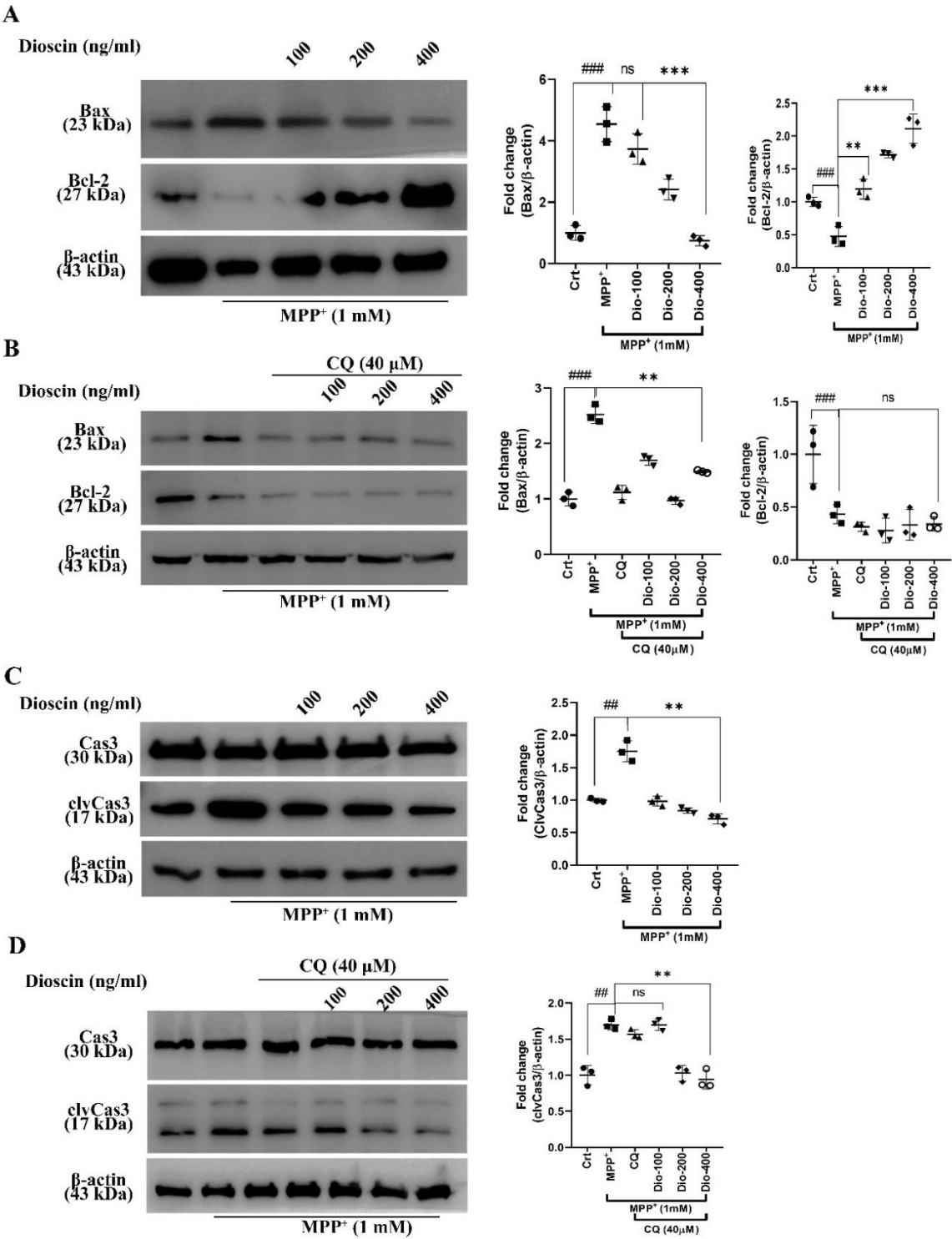
Figure 5: Anti-apoptotic activity of dioscin. Representative data of Bcl-2, Bax (**A & B**) and Cas3/cleaved caspase-3 (**C & D**) immunoblots of whole-cell (SH-SY5Y) lysates. Cells were pre-treated with different doses of dioscin followed by MPP$^+$ (1mM) treatment (**A & C**); cells were pre-treated with CQ 40µM (**B & D**) for autophagic inhibition. The ratio of Bax/Bcl-2 is presented here as fold change against β-actin. The cleaving of clvCas3 from Cas3 is presented as fold changes measured using Image J software. Each WB is representative of 3 independent experiments. The bar graphs represent the ratio of respective protein/β-actin normalised against control (non-treated) samples or MPP$^+$ or MPP$^+$ +CQ-treated cells and are means ± SEM of 3 independent experiments. ns= not significant; $^\#$p<0.05, $^{\#\#}$p<0.01 and $^{\#\#\#}$p<0.001, in comparison to non-treated group; *p<0.05, **p<0.01 and ***p<0.001, compared to toxin and treatment group.

Dioscin dose-dependently increases TH cells and neurotrophic factors

cAMP response element-binding protein (CREB; phosphor/pCREB) is a transcription factor that could modulate the expression of various other transcription factors like cFos, which in extension regulates brain-derived neurotrophic factor (BDNF) translation. As MPP$^+$-induces PD protein aggregation and causes neuronal loss [31], we tested whether or not dioscin-mediated autophagy could rescue neuronal loss via facilitating CREB-dependent BDNF transcription [32]. The result showed a dose-dependent increase in BDNF and pCREB (Fig. 6A). To concrete our hypothesis that autophagosome formation plays a role in dioscin-mediated neuroprotection, we investigated both proteins in the presence of CQ (Fig. 6B). Interestingly, autophagic inhibition restricted dioscin-potentiality in the rescue of neuronal loss (Fig. 6B).

Tyrosine hydroxylase (TH) is the key enzyme for dopaminergic synthesis. Reduction in TH level causes downregulation of dopaminergic synthesis, which is key for motor dysfunction syndrome in PD. We observed that dioscin pre-treatment restores ATG5 level; therefore, we checked

whether it could ameliorate MPP+-mediated TH impairment in SH-SY5Y cell lysates. As the TH

level regards positive biomarkers of dopaminergic synthesis, our findings support the hypothesis

that dioscin promotes dopaminergic neuronal survival (Fig. 6C). And this action might be partly

regulated by its autophagy induction, as we found no significant improvement in the presence of

CQ (Fig. 6D). These results suggest that dioscin treatment enhanced BDNF synthesis, possibly

via facilitating CREB/cFos/BDNF pathway. In contrast, the dioscin-mediated increase in ATG5
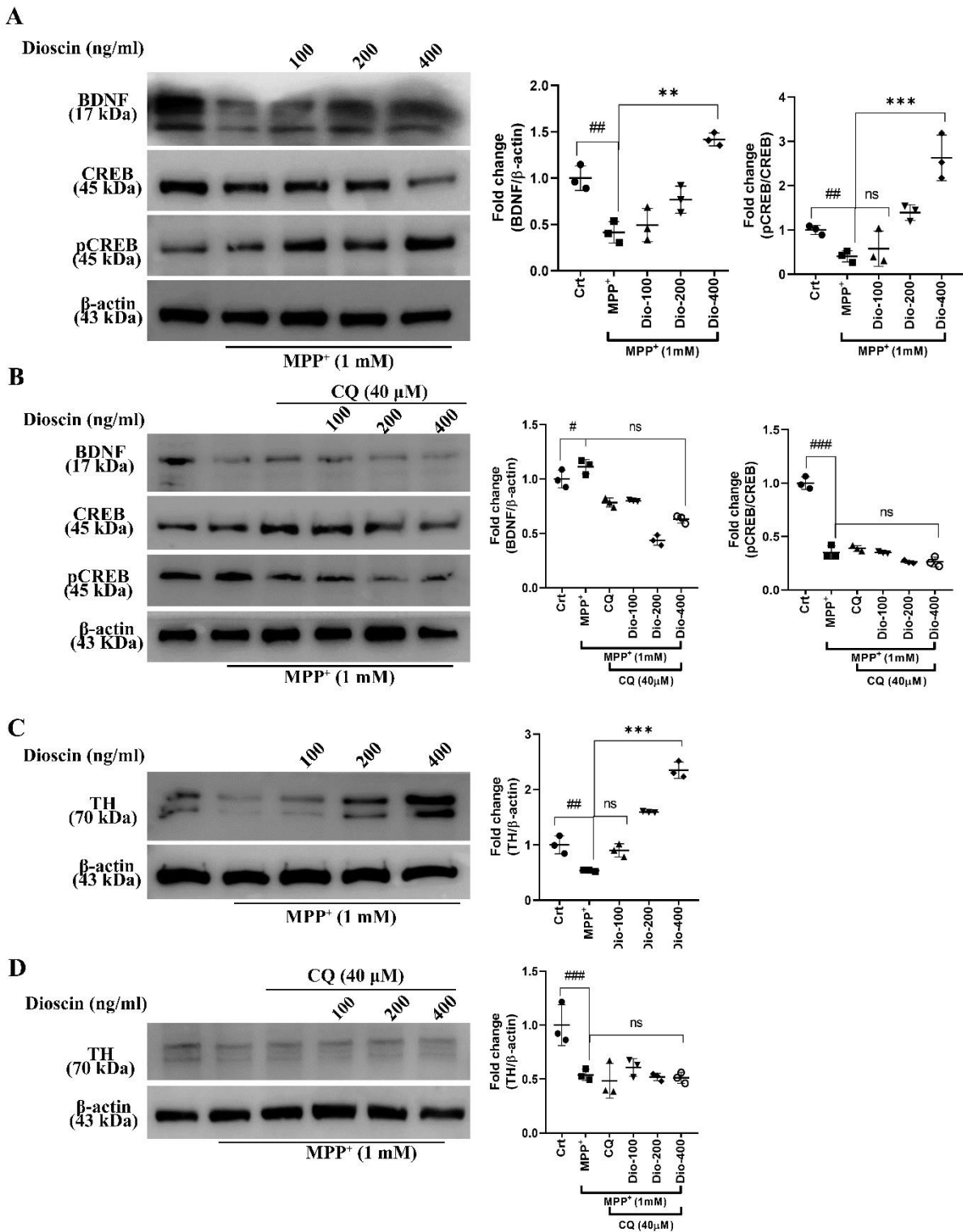
facilitates TH/dopamine levels.

Figure 6: Dioscin improves neurotrophic factors and TH cells. Representative data of TH (**C** & **D**), BDNF, CREB and pCREB (**A** & **B**) immunoblots of whole-cell (SH-SY5Y) lysates. Cells

were pre-treated with different doses of dioscin followed by treatment with MPP$^+$ (1 mM) (**A & C**); cells were pre-treated with CQ (40µM) for autophagic inhibition (**B & D**). Optical density measured using Image J software. Each WB is representative of 3 independent experiments. The bar graphs represent the ratio of respective protein/β-actin or CREB normalised against control (non-treated) samples or MPP$^+$ or MPP$^+$ +CQ-treated cells and are mean ± SEM of 3 independent experiments. ns= not significant; $^#$p<0.05, $^{##}$p<0.01 and $^{###}$p<0.001, in comparison to non-treated group; *p<0.05, **p<0.01 and ***p<0.001, compared to toxin and treatment group.

Discussion

While dioscin-treated autophagy activation demonstrates anti-apoptotic and anti-inflammatory properties, it is not clear whether this activation can protect against neurotoxicity in dopaminergic neurons. Therefore, this study was conducted to examine the role of dioscin-treated activation of autophagy in dopaminergic neuronal cell death.

Mitochondria play a vital role in cellular energy production, and mitochondrial dysfunction has been shown to contribute to different disease pathogenesis, including PD. MPP$^+$ is a commonly used neurotoxin to establish an *in vitro* PD model that inhibits mitochondrial electron transport chain complex I [33]. MPP$^+$ treatment causes elevation of intracellular ROS level, impairs mitochondrial function, and eventually causes cell death via activation of the apoptotic pathway. Chronic exposure to MPP$^+$ deposits into dopamine neurons through a selective uptake by the DAT and induces a PD like a syndrome in cell and animal models [34]. Chronic exposure also impairs autophagic flux [14,35], whereas acute exposure can lead to a transient increase of autophagic flux *in vitro* [35]. Consistent with a previous study [14], this study has found that autophagy reporter protein p62 accumulated and diminished LC3II expression at 24 h of treatment with MPP$^+$.

Earlier findings showed that dioscin exerts neuroprotection against toxicity by activating several mechanisms, including inhibition of inflammatory reactions and release of neurotrophic factors [18]. Dioscin role in autophagy is well studied; most studies conducted on various tumour cell lines [16] indicated dioscin exert activities through PI3k/Akt-dependent or mTOR-dependent pathways [16,19] and reported that the autophagy induced by dioscin is usually caused cell death. A recent study showed that dioscin- autophagy might be involved in the neuroprotective activity in $A\beta_{1-42}$ oligomers treated HT22 cells [17]. The current study supported that result and found that dioscin was found to ameliorate MPP^+-induced autophagic flux impairment.

Mammalian cells impose three primary types of autophagy: macroautophagy, microautophagy and chaperone-mediated autophagy. It is well known that macroautophagy initiates with autophagosome formation, a spherical double-membrane vesicle, which delivers cytoplasmic components into the lysosome. LC3II is a marker of the autophagosome, and the increased expression of LC3II reflects on the formation of the autophagosome. Afterwards, autophagosomes fuse into lysosomes to form autolysosomes and eventually degrade to expel intracellular substrates [8]. Nevertheless, p62 protein starts accumulating when autolysosome degradation is impaired, which remarks the impairment of the autophagy process [35]. This current study investigated the dioscin effect on autophagy markers in the presence of a common autophagy inhibitor, CQ, to ensure dioscin induces autophagy in a mammalian cell line. As an autophagy inhibitor, CQ blocks the delivery of sequestered cargo into lysosomes, impairs autophagic degradation and accumulates autophagosomes [27], which can explain the findings that the presence of CQ upregulated the level of LC3II and p62 expression induced by dioscin. In addition, suppressing ATG5 upregulates p62 accumulation and indicates downregulation of autophagy [36]. ATG5 plays a vital role in canonical and non-canonical autophagy and crosstalk

21

with apoptosis [29]. Dioscin pre-treatment was shown to increase ATG5 expression, which was significantly suppressed by the MPP$^+$ treatment. This effect of dioscin was substantially reversed in the presence of CQ. CQ has no impact on the formation of autophagosomes, but it inhibits the degradation of autophagosomes [27]. Our results suggest activation of autophagy might play a protective role in MPP$^+$-induced activation PD, and dioscin exerted a protective role through inducing autophagy.

It has been shown that PD pathogenesis involves apoptosis and caspase activation that causes dopaminergic cell degeneration [37,38]. MPP$^+$ treatment leads to mitochondrial dysfunction and increases mitochondrial permeability. Eventually, it increases the release of cytochrome c (Cyt C) from mitochondria to plasma, forms apoptosome and leads to activation of caspase-3 [39]. Additionally, Cyt C release is regulated by Bax/Bcl-2 ratio. This study showed that dioscin pre-treatment substantially downregulates the apoptosis pathway by increasing Bcl-2 while decreasing Bax expression, followed by suppressing caspase-3 activation. The inhibition of autophagy reversed the effect. This result indicates that dioscin-induced downregulation of the apoptosis pathway was partially dependent on the autophagy pathway.

Autophagy plays a part in the integrated pro-survival signalling, including AKT/CREB and defect in autophagy led cells toward necrotic death [40]. In this study, our prime focus was on cell survival activity exerted by dioscin, precisely CREB/BDNF expression. Since activation of CREB by the phosphorylation, pCREB binds to the cAMP response element (CRE) site and triggers a gene transcription that includes cFos [32,41-43]. Evidence indicates that cFos is a regulator of BDNF expression and is responsible for the survival and differentiation of neurons [44]. However, BDNF itself can induce cFos transcription in a feedforward cascade [45,46]. MPP$^+$ treatment impairs Ca^{2+} influx, leading to Akt/mTOR pathway inactivation in SH-SY5Y cells that

causes downregulation of BDNF and pCREB and degenerates TH-positive neurons [43,47,48]. Disocin treatment ameliorated cells survivability via increasing BDNF, pCREB and TH expression in the MPP$^+$-treated cellular PD model. In this study, CQ-mediated inhibition of autophagy affected dioscin's activity at various stages; therefore, dioscin-induced effect in BDNF, pCREB and TH expression was investigated in CQ where dioscin showed no protective effect. This finding further indicates that dioscin-mediated neuroprotection is partly regulated through autophagy induction.

Based on the study findings, dioscin ameliorates autophagic flux impairment that might be involved in its neuroprotective effect against MPP$^+$-induced cell apoptosis in the SH-SY5Y neuroblastoma cell line. Further investigation revealed that dioscin upregulates neurotrophic factors and dopamine precursor TH. Altogether, the present findings indicate that the autophagy pathway plays a major role behind dioscin-mediated neuroprotection on SH-SY5Y neuroblastoma cells.

Methods and materials

Chemicals

Dioscin (≥98% purity) was purchased from Chem Faces (Wuhan, Hubei 430056, China), 1-methyl-4-phenylpyridinium (MPP$^+$), chloroquine diphosphate (CQ; C6628), dimethyl sulfoxide (DMSO) and 3-(3,4-dimehylthiazol-2-yl)-2,5-diphenyltetrazolium bromide (MTT) were obtained from Sigma-Aldrich (St. Louis, MO, USA). Foetal bovine serum (FBS) (#16000-442; Gibco, NY14072, USA), phosphate-buffered saline (PBS) and Dulbecco's modified Eagle's medium (DMEM/F12) were purchased from Gibco-BRL Technologies (Gaithersburg, MD, USA). RIPA buffer (10x) was purchased from Millipore (Milford, MA, USA), and protease and phosphatase inhibitors were obtained from Roche (Indianapolis, IN, USA). All other chemicals utilised in this

research were of analytical grade and were purchased unless otherwise noted, from Sigma-Aldrich.

Cell culture and treatment

Human neuroblastoma SH-SY5Y cells were obtained from the American Type Culture Collection (ATCC; Manassas, VA, USA), as mentioned earlier [49]. The neuroblastoma cells were cultured in DMEM/F12 (1:1) supplemented with 100 U/mL penicillin/streptomycin and 10% (v/v) inactivated FBS in an incubator, condition maintained at 37^0C temperature and 5% CO_2. The cells were trypsinised (0.05% trypsin-EDTA) after reaching 80-90% confluence for sub-culture, and the media was replaced every 2 days interval. Each experiment was conducted at least three times from three consecutive passages for statistical analysis.

The SH-SY5Y cells were exposed to MPP$^+$ (1 mM) for 24 h to establish the PD model. During the experiment, different doses of dioscin (100 – 400 ng/ml) were added to SH-SY5Y cells 2 h before the addition of MPP$^+$ (1 mM) and the cells were maintained at 37^0C with 5% CO_2 conditioned incubator. For the study of autophagy, CQ (40 µM) were incubated 1 h before MPP$^+$ treatment.

Cell viability assay

The SH-SY5Y cells were seeded at 2.5×10^5 cells/ml in a 96-well plate to assess viability using the MTT assay method described previously [49,50]. Briefly, cells were incubated for 24 h with a culture medium before treating respective chemicals at the prescribed dose. Cells culture medium was then replaced with medium containing MPP$^+$ (0.25 – 2 mM) or CQ (10 – 40 µM) or MPP$^+$ and dioscin (800 – 50 ng/ml) or CQ, MPP$^+$ and dioscin for another 24 h. Later, 20 µL of MTT (5 mg/ml) was added to each well, and the plate was incubated for an additional 3 h at 37^0C and 5%

CO_2. The medium was then carefully removed using a suction pump, and 200 µL of DMSO was added to each well and shaken for 30 mins to dissolve formazan crystals. The absorption was taken at 552 nm using a microplate reader (Sunrise[TM], Tecan Trading AG, Switzerland).

Western blot analysis

The cells were washed twice with cold PBS and subjected to lyse using lysis buffer (1x RIPA lysis buffer containing protease- and phosphatase inhibitor (1:1) cocktail). Whole mixtures were centrifuged at 14,000 rpm at 4^0C for 15 min, and the supernatants were collected carefully without disturbing pellets. The total protein obtained from cell lysates were quantified using DC[TM] protein assay kit (Bio-Rad, USA) according to manufacturer instruction. Equal amounts of protein (20 µg) were separated electrophoretically using 8~15% sodium dodecyl sulphate-polyacrylamide electrophoresis (SDS-PAGE) gel and then transferred onto polyvinylidene-difluoride (PVDF) membranes (Millipore, Bedford, MA, USA). The membranes were incubated at room temperature for 1 h with 3% bovine serum albumin in Tris-buffered saline (containing 0.1% Tween 20 buffer) to prevent nonspecific binding. Subsequently, the blots were incubated overnight at 4^0C with specific primary antibodies, including anti-Caspase3 (#H-277; santa cruz biotechnology), anti-clvCaspase3 (#9661; cell signaling technology), anti-pCREB (#87G3; cell signaling technology), anti-TH (#ab112; abcam), anti-BDNF (#ab226843; abcam), anti-SQSTM1/p62 (#ab109012; abcam), anti-ATG5 (#ab108327; abcam), anti-Bax (#P-19; santa cruz biotechnology), anti-Bcl-2 (#N-19; santa cruz biotechnology) and anti-LC3 (#ab192890; abcam) at 1:1,000, and anti-β-actin (#C4; santa cruz biotechnology) at 1:5,000 concentration. Next, each blot was incubated at room temperature with either anti-mouse or anti-rabbit (1:10,000) secondary antibody. The blots were visualised with an enhanced chemiluminescence detection system (LAS 500; GE Healthcare Bio-Sciences AB, Sweden) as per the recommended protocol.

Immunofluorescence

The immunocytochemistry was performed as described previously [51]. Briefly, SH-SY5Y cells were grown to a confluency of 70-80%, washed with cold PBS once, followed by fixation with 4% cold PFA for 15 min at room temperature. After discarding PFA, cells were washed (2x) and permeabilised with 0.1% Triton X-100 for 10 min at room temperature prior to blocking with 5%BSA (in 0.1%PBS-Tween 20) for 1 h at room temperature. Cells were then washed and incubated with primary antibody (anti-LC3; #ab192890; abcam) at 2 µg/ml for overnight at 4^0C. The cells were counterstained with chicken-anti-rabbit (CAR-594; A21201 Invitrogen) at 1:400 in 5%BSA for 1 h at room temperature before staining with DAPI (2 µg/ml). Images were immediately captured using Nikon Eclipse Ts2R fluorescence microscopy system and were processed by NIS-Elements BR-2.01.00 software (came with the instrument). Cells were stained with DAPI (2 µg/ml) for apoptosis investigation after fixation and permeabilisation.

Statistical analysis

Statistical analyses were performed using GraphPad Prism (version-8.0.1; La Jolla, CA, USA) software. Data represented as means ± SEM (standard error mean) of three independent experiments. All data were analysed using one-way ANOVA followed by Sidak's multiple comparisons to determine the significance; the p-value was set *<0.05* to be considered statistically significant.

Abbreviations

Parkinson's disease: PD; Dopaminergic: DAergic; Substantia nigra pars compacta: SNpc; Reactive oxygen species: ROS; Dopamine transporter: DAT; 1-methyl-4-phenyl-1,2,3,6-tetrahydropyridine: MPTP; 1-Methyl-4-phenylpyridinium ion: MPP^+; Microtubule-associated protein light-chain 3:

LC3; Sequestosome 1: SQSTM1/p62; Autophagy-related protein: Atg5; B-cell lymphoma 2: Bcl-2; Bcl-2 associated X protein: Bax; Activated Caspase-3: clvCas-3; cAMP response element: CRE; Cytochrome c: Cyt C; Tyrosine hydroxylase: TH; Brain-derived neurotrophic factor: BDNF; Phosphor-cAMP response element-binding protein: pCREB.

Statement & Declaration

Acknowledgements

Conflict of Interests

All authors declare no conflict of interest.

Author contributions

DKC was involved in study designing and supervised the work. SA have done experiments and collected data; SA, MEH, MJ and ISK interpreted all data. SA and MJ wrote the manuscript, and DYC, JSK and ISK have reviewed final draft of the manuscript. Finally, all authors have read and agreed to publish this version of the manuscript.

Data Availability

The datasets generated and/or analysed during current study are publicly available upon acceptance of this manuscript.

References

1.   Haque, M.E.; Akther, M.; Jakaria, M.; Kim, I.S.; Azam, S.; Choi, D.K. Targeting the microglial NLRP3 inflammasome and its role in Parkinson's disease. *Movement disorders : official journal of the Movement Disorder Society* **2020**, *35*, 20-33, doi:10.1002/mds.27874.

2.   Liu, J.; Wang, X.; Lu, Y.; Duan, C.; Gao, G.; Lu, L.; Yang, H. Pink1 interacts with α-synuclein and abrogates α-synuclein-induced neurotoxicity by activating autophagy. *Cell death & disease* **2017**, *8*, e3056, doi:10.1038/cddis.2017.427.

3.   Franco-Iborra, S.; Vila, M.; Perier, C. The Parkinson Disease Mitochondrial Hypothesis: Where Are We at? *The Neuroscientist : a review journal bringing neurobiology, neurology and psychiatry* **2016**, *22*, 266-277, doi:10.1177/1073858415574600.

4.   Jakaria, M.; Park, S.-Y.; Haque, M.E.; Karthivashan, G.; Kim, I.-S.; Ganesan, P.; Choi, D.-K. Neurotoxic Agent-Induced Injury in Neurodegenerative Disease Model: Focus on Involvement of Glutamate Receptors. *Front Mol Neurosci* **2018**, *11*, 307-307, doi:10.3389/fnmol.2018.00307.

5.   Langston, J.W.; Ballard, P.; Tetrud, J.W.; Irwin, I. Chronic Parkinsonism in humans due to a product of meperidine-analog synthesis. *Science (New York, N.Y.)* **1983**, *219*, 979-980, doi:10.1126/science.6823561.

6.   Dauer, W.; Przedborski, S. Parkinson's disease: mechanisms and models. *Neuron* **2003**, *39*, 889-909, doi:10.1016/s0896-6273(03)00568-3.

7.   Cuervo, A.M. Autophagy: many paths to the same end. *Molecular and cellular biochemistry* **2004**, *263*, 55-72.

8.   Kobayashi, S. Choose Delicately and Reuse Adequately: The Newly Revealed Process of Autophagy. *Biological & pharmaceutical bulletin* **2015**, *38*, 1098-1103, doi:10.1248/bpb.b15-00096.

9.   Patel, A.S.; Lin, L.; Geyer, A.; Haspel, J.A.; An, C.H.; Cao, J.; Rosas, I.O.; Morse, D. Autophagy in idiopathic pulmonary fibrosis. *PloS one* **2012**, *7*, e41394, doi:10.1371/journal.pone.0041394.

10.   Levine, B.; Kroemer, G. Autophagy in the pathogenesis of disease. *Cell* **2008**, *132*, 27-42, doi:10.1016/j.cell.2007.12.018.

11.   Friedman, L.G.; Lachenmayer, M.L.; Wang, J.; He, L.; Poulose, S.M.; Komatsu, M.; Holstein, G.R.; Yue, Z. Disrupted autophagy leads to dopaminergic axon and dendrite degeneration and promotes presynaptic accumulation of α-synuclein and LRRK2 in the brain. *The Journal of neuroscience : the official journal of the Society for Neuroscience* **2012**, *32*, 7585-7593, doi:10.1523/jneurosci.5809-11.2012.

12.   Prommahom, A.; Dharmasaroja, P. Effects of eEF1A2 knockdown on autophagy in an MPP(+)-induced cellular model of Parkinson's disease. *Neuroscience research* **2021**, *164*, 55-69, doi:10.1016/j.neures.2020.03.013.

13.   Ramalingam, M.; Kim, S.J. Insulin on activation of autophagy with integrins and syndecans against MPP(+)-induced α-synuclein neurotoxicity. *Neuroscience letters* **2016**, *633*, 94-100, doi:10.1016/j.neulet.2016.09.023.

14.   Zhang, Y.; Wu, J.Y.; Weng, L.H.; Li, X.X.; Yu, L.J.; Xu, Y. Valproic acid protects against MPP(+)-mediated neurotoxicity in SH-SY5Y Cells through autophagy. *Neuroscience letters* **2017**, *638*, 60-68, doi:10.1016/j.neulet.2016.12.017.

15.   Garcia-Garcia, A.; Anandhan, A.; Burns, M.; Chen, H.; Zhou, Y.; Franco, R. Impairment of Atg5-dependent autophagic flux promotes paraquat- and MPP$^+$-induced apoptosis but not rotenone or 6-hydroxydopamine toxicity. *Toxicological sciences : an official journal of the Society of Toxicology* **2013**, *136*, 166-182, doi:10.1093/toxsci/kft188.

16.   Hsieh, M.J.; Tsai, T.L.; Hsieh, Y.S.; Wang, C.J.; Chiou, H.L. Dioscin-induced autophagy mitigates cell apoptosis through modulation of PI3K/Akt and ERK and JNK signaling pathways in human lung cancer cell lines. *Archives of toxicology* **2013**, *87*, 1927-1937, doi:10.1007/s00204-013-1047-z.

17.   Zhang, Z.; Han, K.; Wang, C.; Sun, C.; Jia, N. Dioscin Protects against Aβ1-42 Oligomers-Induced Neurotoxicity via the Function of SIRT3 and Autophagy. *Chemical & pharmaceutical bulletin* **2020**, *68*, 717-725, doi:10.1248/cpb.c20-00046.

18.   Qi, Y.; Li, R.; Xu, L.; Yin, L.; Xu, Y.; Han, X.; Peng, J. Neuroprotective Effect of Dioscin on the Aging Brain. *Molecules (Basel, Switzerland)* **2019**, *24*, doi:10.3390/molecules24071247.

19.   Du, S.; Li, C.; Lu, Y.; Lei, X.; Zhang, Y.; Li, S.; Liu, F.; Chen, Y.; Weng, D.; Chen, J. Dioscin Alleviates Crystalline Silica-Induced Pulmonary Inflammation and Fibrosis through Promoting Alveolar Macrophage Autophagy. *Theranostics* **2019**, *9*, 1878-1892, doi:10.7150/thno.29682.

20.   Zhu, S.; Tang, S.; Su, F. Dioscin inhibits ischemic stroke-induced inflammation through inhibition of the TLR4/MyD88/NF-κB signaling pathway in a rat model. *Molecular medicine reports* **2018**, *17*, 660-666, doi:10.3892/mmr.2017.7900.

21.   Yang, R.; Chen, W.; Lu, Y.; Li, Y.; Du, H.; Gao, S.; Dong, X.; Yuan, H. Dioscin relieves endotoxemia induced acute neuro-inflammation and protect neurogenesis via improving 5-HT metabolism. *Scientific Reports* **2017**, *7*, 40035, doi:10.1038/srep40035.

22.   Wang, Z.; Du, Q.; Wang, F.; Liu, Z.; Li, B.; Wang, A.; Wang, Y. Microarray analysis of gene expression on herbal glycoside recipes improving deficient ability of spatial learning memory in ischemic mice. *Journal of neurochemistry* **2004**, *88*, 1406-1415, doi:10.1046/j.1471-4159.2003.02258.x.

23.   Hu, Z.Y.; Chen, B.; Zhang, J.P.; Ma, Y.Y. Up-regulation of autophagy-related gene 5 (ATG5) protects dopaminergic neurons in a zebrafish model of Parkinson's disease. *The Journal of biological chemistry* **2017**, *292*, 18062-18074, doi:10.1074/jbc.M116.764795.

24.   Hu, Z.; Zhang, J.; Zhang, Q. Expression pattern and functions of autophagy-related gene atg5 in zebrafish organogenesis. *Autophagy* **2011**, *7*, 1514-1527, doi:10.4161/auto.7.12.18040.

25.   Khwanraj, K.; Phruksaniyom, C.; Madlah, S.; Dharmasaroja, P. Differential Expression of Tyrosine Hydroxylase Protein and Apoptosis-Related Genes in Differentiated and Undifferentiated SH-SY5Y Neuroblastoma Cells Treated with MPP(.). *Neurology research international* **2015**, *2015*, 734703, doi:10.1155/2015/734703.

26.   Fan, F.; Li, S.; Wen, Z.; Ye, Q.; Chen, X.; Ye, Q. Regulation of PGC-1α mediated by acetylation and phosphorylation in MPP+ induced cell model of Parkinson's disease. *Aging* **2020**, *12*, 9461-9474, doi:10.18632/aging.103219.

27.   Mauthe, M.; Orhon, I.; Rocchi, C.; Zhou, X.; Luhr, M.; Hijlkema, K.J.; Coppes, R.P.; Engedal, N.; Mari, M.; Reggiori, F. Chloroquine inhibits autophagic flux by decreasing autophagosome-lysosome fusion. *Autophagy* **2018**, *14*, 1435-1455, doi:10.1080/15548627.2018.1474314.

28.   Jia, B.; Xue, Y.; Yan, X.; Li, J.; Wu, Y.; Guo, R.; Zhang, J.; Zhang, L.; Li, Y.; Liu, Y., et al. Autophagy inhibitor chloroquine induces apoptosis of cholangiocarcinoma cells via endoplasmic reticulum stress. *Oncology letters* **2018**, *16*, 3509-3516, doi:10.3892/ol.2018.9131.

29.   Ye, X.; Zhou, X.J.; Zhang, H. Exploring the Role of Autophagy-Related Gene 5 (ATG5) Yields Important Insights Into Autophagy in Autoimmune/Autoinflammatory Diseases. *Frontiers in immunology* **2018**, *9*, 2334, doi:10.3389/fimmu.2018.02334.

30.   Lei, Z.; Cao, G.; Wei, G. A30P mutant α-synuclein impairs autophagic flux by inactivating JNK signaling to enhance ZKSCAN3 activity in midbrain dopaminergic neurons. *Cell death & disease* **2019**, *10*, 133, doi:10.1038/s41419-019-1364-0.

31.   Kalivendi, S.V.; Cunningham, S.; Kotamraju, S.; Joseph, J.; Hillard, C.J.; Kalyanaraman, B. Alpha-synuclein up-regulation and aggregation during MPP+-induced apoptosis in neuroblastoma cells: intermediacy of transferrin receptor iron and hydrogen peroxide. *The Journal of biological chemistry* **2004**, *279*, 15240-15247, doi:10.1074/jbc.M312497200.

32.   Abd-Elrahman, K.S.; Ferguson, S.S.G. Modulation of mTOR and CREB pathways following mGluR5 blockade contribute to improved Huntington's pathology in zQ175 mice. *Molecular Brain* **2019**, *12*, 35, doi:10.1186/s13041-019-0456-1.

33.   Singer, T.P.; Ramsay, R.R. Mechanism of the neurotoxicity of MPTP. An update. *FEBS letters* **1990**, *274*, 1-8, doi:10.1016/0014-5793(90)81315-f.

34.   Eberhardt, O.; Schulz, J.B. Apoptotic mechanisms and antiapoptotic therapy in the MPTP model of Parkinson's disease. *Toxicology letters* **2003**, *139*, 135-151, doi:10.1016/s0378-4274(02)00428-9.

35. Lim, J.; Kim, H.W.; Youdim, M.B.; Rhyu, I.J.; Choe, K.M.; Oh, Y.J. Binding preference of p62 towards LC3-ll during dopaminergic neurotoxin-induced impairment of autophagic flux. *Autophagy* **2011**, *7*, 51-60, doi:10.4161/auto.7.1.13909.

36. Mizushima, N.; Yoshimori, T. How to interpret LC3 immunoblotting. *Autophagy* **2007**, *3*, 542-545, doi:10.4161/auto.4600.

37. Turmel, H.; Hartmann, A.; Parain, K.; Douhou, A.; Srinivasan, A.; Agid, Y.; Hirsch, E.C. Caspase-3 activation in 1-methyl-4-phenyl-1,2,3,6-tetrahydropyridine (MPTP)-treated mice. *Movement disorders : official journal of the Movement Disorder Society* **2001**, *16*, 185-189, doi:10.1002/mds.1037.

38. Gómez, C.; Reiriz, J.; Piqué, M.; Gil, J.; Ferrer, I.; Ambrosio, S. Low concentrations of 1-methyl-4-phenylpyridinium ion induce caspase-mediated apoptosis in human SH-SY5Y neuroblastoma cells. *Journal of neuroscience research* **2001**, *63*, 421-428, doi:10.1002/1097-4547(20010301)63:5<421::Aid-jnr1037>3.0.Co;2-4.

39. Friedlander, R.M. Apoptosis and caspases in neurodegenerative diseases. *The New England journal of medicine* **2003**, *348*, 1365-1375, doi:10.1056/NEJMra022366.

40. Carloni, S.; Girelli, S.; Scopa, C.; Buonocore, G.; Longini, M.; Balduini, W. Activation of autophagy and Akt/CREB signaling play an equivalent role in the neuroprotective effect of rapamycin in neonatal hypoxia-ischemia. *Autophagy* **2010**, *6*, 366-377, doi:10.4161/auto.6.3.11261.

41. Gandolfi, D.; Cerri, S.; Mapelli, J.; Polimeni, M.; Tritto, S.; Fuzzati-Armentero, M.T.; Bigiani, A.; Blandini, F.; Mapelli, L.; D'Angelo, E. Activation of the CREB/c-Fos Pathway during Long-Term Synaptic Plasticity in the Cerebellum Granular Layer. *Frontiers in cellular neuroscience* **2017**, *11*, 184, doi:10.3389/fncel.2017.00184.

42. Saura, C.A.; Cardinaux, J.R. Emerging Roles of CREB-Regulated Transcription Coactivators in Brain Physiology and Pathology. *Trends in neurosciences* **2017**, *40*, 720-733, doi:10.1016/j.tins.2017.10.002.

43. Tao, X.; Finkbeiner, S.; Arnold, D.B.; Shaywitz, A.J.; Greenberg, M.E. Ca2+ influx regulates BDNF transcription by a CREB family transcription factor-dependent mechanism. *Neuron* **1998**, *20*, 709-726, doi:10.1016/s0896-6273(00)81010-7.

44. Dong, M.; Wu, Y.; Fan, Y.; Xu, M.; Zhang, J. c-fos modulates brain-derived neurotrophic factor mRNA expression in mouse hippocampal CA3 and dentate gyrus neurons. *Neuroscience letters* **2006**, *400*, 177-180, doi:10.1016/j.neulet.2006.02.063.

45. Zhang, J.; Zhang, D.; McQuade, J.S.; Behbehani, M.; Tsien, J.Z.; Xu, M. c-fos regulates neuronal excitability and survival. *Nature genetics* **2002**, *30*, 416-420, doi:10.1038/ng859.

46. Lipsky, R.H.; Marini, A.M. Brain-derived neurotrophic factor in neuronal survival and behavior-related plasticity. *Annals of the New York Academy of Sciences* **2007**, *1122*, 130-143, doi:10.1196/annals.1403.009.

47. Selvaraj, S.; Sun, Y.; Watt, J.A.; Wang, S.; Lei, S.; Birnbaumer, L.; Singh, B.B. Neurotoxin-induced ER stress in mouse dopaminergic neurons involves downregulation of TRPC1 and inhibition of AKT/mTOR signaling. *The Journal of clinical investigation* **2012**, *122*, 1354-1367, doi:10.1172/jci61332.

48. Nam, J.H.; Leem, E.; Jeon, M.T.; Jeong, K.H.; Park, J.W.; Jung, U.J.; Kholodilov, N.; Burke, R.E.; Jin, B.K.; Kim, S.R. Induction of GDNF and BDNF by hRheb(S16H) transduction of SNpc neurons: neuroprotective mechanisms of hRheb(S16H) in a model of Parkinson's disease. *Molecular neurobiology* **2015**, *51*, 487-499, doi:10.1007/s12035-014-8729-2.

49. Haque, M.E.; Akther, M.; Azam, S.; Choi, D.K.; Kim, I.S. GPR4 Knockout Improves the Neurotoxin-Induced, Caspase-Dependent Mitochondrial Apoptosis of the Dopaminergic Neuronal Cell. *International journal of molecular sciences* **2020**, *21*, doi:10.3390/ijms21207517.

50. Jakaria, M.; Azam, S.; Cho, D.Y.; Haque, M.E.; Kim, I.S.; Choi, D.K. The Methanol Extract of Allium cepa L. Protects Inflammatory Markers in LPS-Induced BV-2 Microglial Cells and Upregulates the Antiapoptotic Gene and Antioxidant Enzymes in N27-A Cells. *Antioxidants (Basel, Switzerland)* **2019**, *8*, doi:10.3390/antiox8090348.

51. Runwal, G.; Stamatakou, E.; Siddiqi, F.H.; Puri, C.; Zhu, Y.; Rubinsztein, D.C. LC3-positive structures are prominent in autophagy-deficient cells. *Sci Rep* **2019**, *9*, 10147, doi:10.1038/s41598-019-46657-z.